JOURNAL OF MATERIALS SCIENCE 24 (1989) 4379–4386

Chemical reactions between magnesia and aluminium orthophosphate to form magnesia–phosphate cements

T. FINCH
Central Research Laboratories, Thorn EMI, Dawley Road, Hayes, Middlesex, UB3 1HH, UK
J. H. SHARP
School of Materials, University of Sheffield, Northumberland Road, Sheffield, S10 2TZ, UK

The reaction between magnesia and commercial aluminium orthophosphate (AOP) is an exothermic, acid–base reaction leading to an insoluble product, which is a set cement of moderate strength. The products of this reaction are crystalline newberyite, $MgHPO_4 \cdot 3H_2O$, and an amorphous phase. They have been characterized by means of X-ray diffraction, infrared spectroscopy, scanning electron microscopy and various methods of thermal analysis. As the molar ratio of MgO:AOP increases, the cement sets faster with a greater evolution of heat, and the reaction product contains a substantial amount of unreacted MgO. A set of "in-house" acid sources has been prepared which can also lead to the formation of newberyite or to a previously unreported hydrate. The conditions of formation of this hydrate have been investigated and it has been characterized leading to speculation about its composition.

1. Introduction

Metal phosphates are of interest in the ceramics industry for two reasons. Phosphate bonding can lead to good refractoriness because of the high melting points of many metal phosphates. Some of these systems also develop hydraulic bonds at ambient temperatures which have been exploited in dental cements and newer cements recommended particularly for repairs to damaged concrete. The purpose of the present work was to exploit both of these properties to develop a relatively cheap material, that could be injection moulded. Products would have some green strength which would not be completely lost on heating to moderate temperatures (e.g. 1000° C).

A classic series of papers on phosphate bonding was published by Kingery [1] and a useful review by Cassidy [2]. These papers refer to a wide range of compositions of bonding materials, to be used in a variety of applications. The current work concerns the use of aluminium acid phosphates combined with magnesia which gives rise to cold-setting or "castable" cements. As such, the most relevant previous study is that by Ando *et al.* [3]. There are, however, a number of significant differences between that work and the present study, principally that the systems investigated by Ando *et al.* contain less magnesium and more aluminium than ours, as highlighted in Table. I.

The use of excess MgO in our systems makes them more similar to the rapid hardening cements [4–12] for which the name magnesia–phosphate cements has been proposed. The name is intended to cover a group of cements in which unreacted particles of MgO are bonded together in a matrix of hydrated phosphate phases. The latter are often based on struvite, $NH_4MgPO_4 \cdot 6H_2O$, but there is no reason why NH_4^+ ions must be present; indeed the possibility of mixtures involving ammonium magnesium phosphate hydrates and magnesium phosphate hydrates has already been envisaged [8], and a rapid hardening system involving no ammonium at all investigated briefly [9]. The hydrates discussed in the present paper are certainly ammonia-free but they fall well into the general category.

In spite of these previous studies, the chemistry of hydrated metal phosphates is still poorly understood because of their complexity. In the present paper we describe the reactions observed when magnesia powder is added to various acid sources, notably aluminium orthophosphate, $Al(H_2PO_4)_3$. The range of compositions which are discussed below has not been studied by previous workers.

2. Experimental procedure

The MgO used in this work was obtained from Steetley Chemicals, Hartlepool, under the trade name HMD4. It consisted of 96% MgO, dead burnt, with 65% of the particles being less than 53 μm diameter.

Where the term "AOP" is used in the text, it refers specifically to a solution obtained from Albright and

TABLE I Comparison of relative atomic quantities used by Ando [3], and in the current work

	Mg	P	Al	H_2O
Ando *et al.*	0–2	1–3	1	19–36
Current work	2–10	3–4	1	$\geqslant 5.8$

0022–2461/89 $03.00 + .12

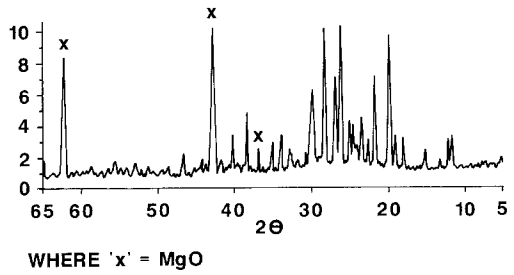

Figure 1 X-ray diffraction pattern for product of reaction between MgO + H_3PO_4.

Wilson, Oldbury. This is a 48% wt/wt solution of AOP in water where "AOP" has the nominal composition of $Al(H_2PO_4)_3$, although some variation in P:Al ratio may occur between batches. Any given batch is probably comprised of a number of different aluminium acid phosphates [2], for example:

$$Al(H_2PO_4)_3 \quad (P:Al = 3:1)$$

$$AlH_3(PO_4)_2 \cdot 3H_2O \quad (P:Al = 2:1)$$

$$Al_2(HPO_4)_3 \quad (P:Al = 3:2)$$

Phosphoric acid was obtained from Albright and Wilson, Oldbury and consisted of 85.3% wt/wt H_3PO_4 in water, with a specific gravity of 1.70. Gibbsite was obtained from B.A. Chemicals, Gerrards Cross under the trade name FRF85, with a purity of 99.6% wt/wt $Al(OH)_3$, and a mean particle diameter of 5 μm.

It will be shown below that a major reaction product was newberyite, $MgHPO_4 \cdot 3H_2O$, which was compared with a relatively pure sample supplied by BDH Chemicals, Poole. X-ray diffraction (XRD) analysis indicated that the BDH newberyite was pure, except that it contained a small quantity of $Mg(OH)_2$.

Samples ($\sim$ 200 g) of set cement were fabricated at 22 $\pm$ 2°C by using spatulation to intimately mix magnesia powder and liquid acids. Spatulation had to be continued almost to the stage when the material became too stiff to manipulate. If stirring was stopped too soon, the reactants tended to separate out on setting and an inhomogenous material resulted.

The X-ray diffraction (XRD) work made use of a Philips diffractometer comprised of a PW1730 generator and a PW1050 goniometer with a graphite monochromator. Cu$K\alpha$ radiation was used at 50 kV, 30 mA with a typical scan speed of 2° min^{-1}. Infrared (IR) spectroscopy was conducted on KBr using a Perkin Elmer 683 IR spectrometer.

Differential scanning calorimetry (DSC) was conducted using a Perkin Elmer DSC-4 unit, and thermogravimetry (TG) using a Perkin Elmer TGS-2, both in conjunction with a PE TADs data station. The runs were conducted on $\sim$ 10 mg samples under an atmosphere of flowing dry nitrogen. Scanning electron microscopy (SEM) was used to examine fractured surfaces and was carried out on a Jeol JSM 840.

TABLE II The seven strongest peaks from Fig. 1 compared with data concerning $Mg(H_2PO_4)_2 \cdot nH_2O$

Data from Fig. 1		$Mg(H_2PO_4)_2 \cdot 2H_2O$ [14]		$Mg(H_2PO_4)_2$ [15]	
d (nm)	*I*	*d* (nm)	*I*	*d* (nm)	*I*
0.339	>100	0.341	93	0.337	80
0.315	>100	0.317	100	0.314	100
0.448	97	0.450	91	0.447	60
0.408	71	0.410	32	0.408	50
0.332	70	0.334	59	–	–
0.299	62	0.301	49	0.298	60
0.234	48	0.235	33	0.233	70

3. Reaction between MgO + H_3PO_4

When magnesia powder was added to phosphoric acid to give a 1:1 molar ratio, a violent, exothermic reaction was observed as reported by Kingery [1]. Although the product of the reaction was hard, it was found to be soluble in water and therefore of limited commercial application.

XRD patterns of the reaction products (Fig. 1) indicate that instead of Reaction 1, which might have been expected, Reaction 2 was followed

$$MgO + H_3PO_4 + 2H_2O \rightarrow MgHPO_4 \cdot 3H_2O \quad (1)$$

$$2MgO + 2H_3PO_4 + H_2O \rightarrow Mg(H_2PO_4) \cdot 2H_2O + MgO \quad (2)$$

At least two highly crystalline phases are clearly present in Fig. 1 along with a phase that is amorphous to X-rays, indicated by the broad "hump" in the background to the pattern between 15° and 35° 2θ with a maximum around 26° 2θ. Substantial amounts of MgO (marked in Fig. 1) are present in accordance with Equation 2. The seven strongest peaks other than those for MgO [13], are listed in order of decreasing intensity in Table II and compared with the data from Hinsch [14] for $Mg(H_2PO_4)_2 \cdot 2H_2O$. The *d*-spacings are in close agreement and the relative intensities in reasonably good agreement. The JCPDS listing [15] for anhydrous $Mg(H_2PO_4)_2$ is also shown in Table II and is very similar, but it draws on data obtained in 1927 and may, therefore, relate to the dihydrate. The XRD patterns reported by Ahmed [16] for $Mg(H_2PO_4)$, $Mg(H_2PO_4) \cdot 2H_2O$ and $Mg(H_2PO_4) \cdot 4H_2O$ are quite different and must be regarded as suspect.

There are also several unassigned peaks present in Fig. 1, as given in Table III. There is therefore a further, as yet unidentified, phase present, which is probably another hydrate, maybe $Mg(H_2PO_4) \cdot 4H_2O$. There is no evidence for the presence of $MgHPO_4 \cdot nH_2O$, $Mg_3(PO_4)_2 \cdot nH_2O$ or $Mg(OH)_2$.

4. Reaction between MgO and commercial $Al(H_2PO_4)_3$

4.1. Characterization of the reaction products

The reaction between MgO and commercial AOP is exothermic and yields a hard, insoluble product which

TABLE III Unassigned XRD peaks produced by the reaction of MgO + H_3PO_4

d (nm)	*I* (uncorrected)
0.763	32
0.734	30
0.676	18
0.394	30
0.357	42
0.292	22
0.283 (br)	17

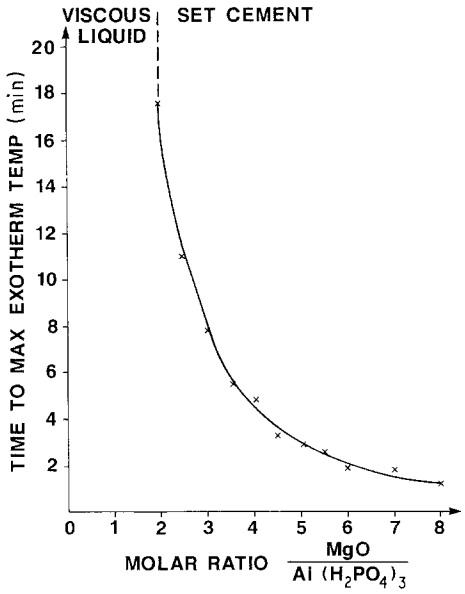

Figure 2 Plot of time to reach maximum exotherm temperature against molar ratio MgO : AOP.

maintains structural integrity to moderately high temperatures (> 1000° C).

As the molar ratio MgO:AOP increased, the cement set faster and with a larger evolution of heat. The time taken to reach the maximum exotherm temperature (which provides an estimate of the setting time) is plotted against the MgO:AOP ratio in Fig. 2. It can be seen that mixtures with an MgO:AOP ratio of less than two failed to produce set cements. At a ratio of exactly two, the mixture "set", but only slowly and always remained tacky.

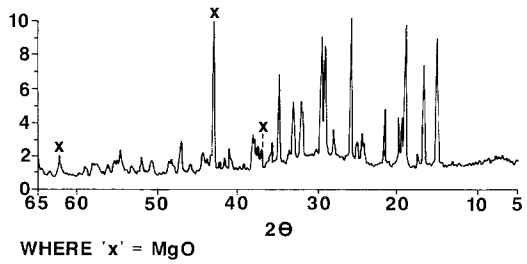

Figure 3 XRD pattern of a cement containing newberyite.

On analysis by XRD, these phosphate cements have been found to contain both crystalline and amorphous phases (Fig. 3). As with Fig. 1, the presence of an amorphous phase is clearly indicated by a hump in the XRD pattern between 20° and 35° 2θ. The sharp peaks on the XRD trace have been identified as due to the presence of two distinct crystalline phases, newberyite, $MgHPO_4 \cdot 3H_2O$, and MgO. The data obtained, with the MgO peaks omitted, are compared in Table IV with the three patterns for newberyite listed in the JCPDS files. The *d*-spacings of our newberyite peaks agree very closely with the standard patterns, and can be completely indexed on an orthorhombic cell with $a = 1.0207$ nm, $b = 1.0681$ nm and $c = 1.0014$ nm. The relative intensities of the three literature traces differ significantly; our intensities agree well with those calculated by Sutor [17]. Also included in Table IV is the XRD pattern of a sample of commercial newberyite (ex-BDH), which gives identical *d*-spacings and a similar set of intensities to the newberyite present in the cements.

The relative amounts of the crystalline materials

TABLE IV Comparison of five sets of data for newberyite

Data from Fig. 3		JCPDS 35-788		JCDPDS 20-153		JCPDS 19-762		Newberyite ex-BDH	
d (nm)	I/I_0	*d* (nm)	I/I_0	*d* (nm)	I/I_0	*d* (nm)	I/I_0	*d* (nm)	I/I_0
0.595	76	0.595	52	0.594	100	0.594	30	0.595	89
0.534	61	0.534	22	0.534	60	0.534	100	0.534	64
0.510	10	0.510	4	0.510	9	0.510	5	0.510	9
0.472	87	0.471	47	0.471	95	0.471	60	0.472	89
0.461	31	0.461	16	0.461	28	0.460	20	0.461	29
0.450	31	0.450	41	0.449	37	0.449	10	0.450	46
0.415	34	0.415	33	0.415	35	0.414	10	0.415	44
0.369	13	0.365	12	0.369	12	0.369	10	0.369	16
0.366	18	–	–	0.365	14	0.365	5	0.366	20
0.358	13	0.357	11	0.358	13	0.357	5	0.358	19
0.345	100	0.346	66	0.346	81	0.346	40	0.345	85
–	–	0.344	33	0.344	22	0.344	10	–	–
0.319	17	0.319	10	0.319	15	0.319	20	0.319	20
0.308	65	0.309	54	0.309	55	0.308	40	0.308	100
0.304	70	0.304	100	0.304	66	0.304	30	0.304	100
0.298	7	0.297	3	–	–	–	–	0.298	6
0.281	28	0.282	24	0.282	18	0.281	10	0.281	35
0.280	33	0.279	22	0.279	26	0.279	20	0.280	35
0.272	36	0.272	32	0.272	30	0.272	20	0.272	51
0.268	8	0.270	13	0.267	5	0.267	20	0.268	8
0.258	54	0.258	34	0.258	35	0.258	40	0.258	52
0.255	6	–	–	–	–	–	–	0.255	6
0.253	15	0.252	11	0.252	11	0.252	10	0.253	15
0.251	9	–	–	–	–	–	–	0.251	10
0.249	5	–	–	0.250	5	0.250	10	0.249	9
0.244	13	0.243	22	–	–	–	–	0.244	15
0.241	14	–	–	0.241	10	0.241	10	0.241	16
0.239	17	–	–	0.239	12	0.239	10	0.239	18
0.237	20	0.237	22	0.237	13	0.237	10	0.237	23

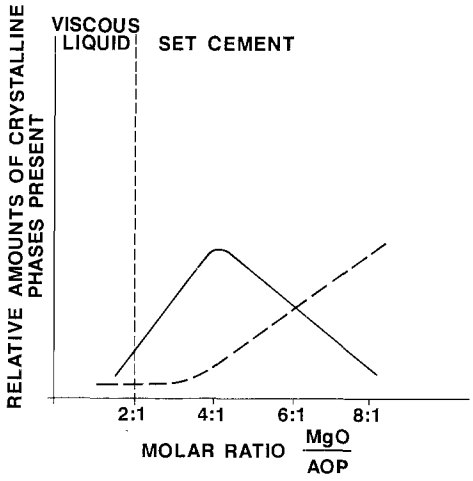

Figure 4 Plot of relative amounts of crystalline phases against molar ratio MgO:AOP. (——) $MgHPO_4 \cdot 3H_2O$, (– – –) MgO.

present in the set cements depended largely on the molar ratio of MgO:AOP used as starting materials as shown in Fig. 4. A maximum amount of newberyite is associated with a molar ratio of about 4:1.

As can be seen from the IR spectrum shown in Fig. 5a, newberyite ex-BDH is a crystalline material, giving rise to numerous, fairly sharp peaks. The peaks between 500 and 1250 cm^{-1} are characteristic of PO_4 bonding [18]. The remaining peaks are indicative of the presence of water of crystallization, especially those at ~3400 and 1640 cm^{-1}. Thus we can see that the pattern in Fig. 5a is that of a crystalline, hydrated phosphate. Reference to standard IR spectra of minerals [18–20] confirms that this trace is closely similar to those reported for newberyite.

The IR spectrum obtained from a typical MgO:AOP cement, which is known to contain newberyite, is shown in Fig. 5b. As can be seen, a similar spectrum to that shown in Fig. 5a was obtained, with perhaps slightly less crystallinity evident in Fig. 5b.

DSC and TG curves of newberyite ex-BDH and one of our reaction products (typical of many obtained) are shown in Figs 6 and 7, respectively. Comparison of these curves indicates that the dehydration of newberyite is responsible for the endotherm and loss in mass at ~160° C (variable with sample mass and heating rate).

Also apparent in Fig. 6b is a second, broad endotherm ~70°, which was always observed in the DSC

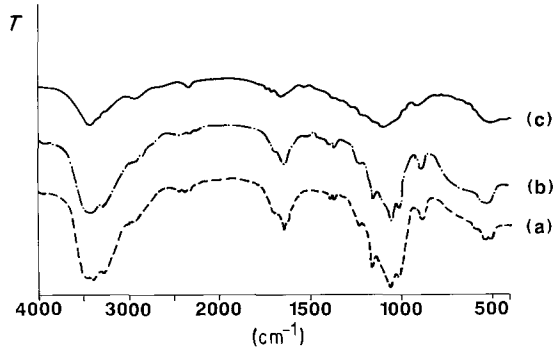

Figure 5 Infrared spectra of (a) newberyite ex-BDH, (b) a cement containing newberyite, (c) a cement containing hayesite.

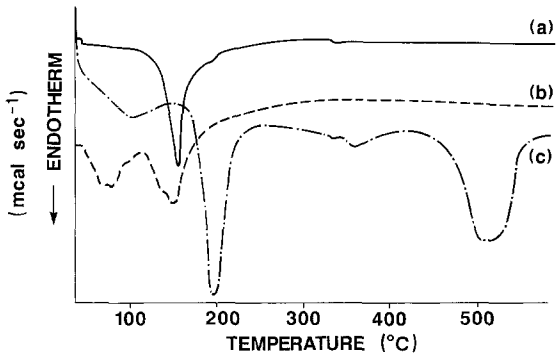

Figure 6 DSC curves of (a) newberyite ex-BDH, (b) a cement containing newberyite, (c) a cement containing hayesite.

curves of the cements but was absent in that of the samples of BDH newberyite. This low-temperature endotherm, which has an associated loss in mass shown in Fig. 7b, is attributed to the dehydration of the amorphous phase. This may be a hydrate or a gel-like material with adsorbed water in microscopic pores. Because aluminium and phosphorus are the elements adjacent to silicon in the Periodic Table, silica gel may represent a model for this phase.

A further hydrate was identified after a set cement had been suspended in water and subsequently dried slowly in air at ambient temperatures. The XRD and DSC traces of a sample of this material are shown in Figs 8 and 9, respectively. The XRD data correspond closely [21] to a mixture of newberyite and phosphorresslerite, $Mg\ HPO_4 \cdot 7H_2O$. The DSC curve (Fig. 9a) shows a major endothermic reaction below 100° C and little evidence for the intermediate formation of newberyite. On ageing at room temperature, however, phosphorreslerite readily transforms into newberyite, as indicated by a DSC curve on the same material after two weeks at ambient conditions (Fig. 9b). This observation is in accordance with that reported by Van Wazer [22], Rassonskaya and Novikova [23], and Lehr *et al.* [20].

The low-temperature endotherm seen in the DSC curve of the set cement (Fig. 6b) cannot, however, be attributed to the presence of the heptahydrate, because XRD patterns of samples that gave such DSC curves never showed any evidence for the presence of this phase.

4.2. Stoichiometry of the reaction

Because neither of the crystalline phases present in the cements contains aluminium, it is assumed that all of the aluminium introduced from AOP is present in the

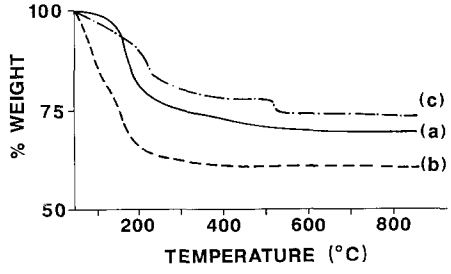

Figure 7 TG curves of (a) newberyite ex-BDH, (b) a cement containing newberyite, (c) a cement containing hayesite.

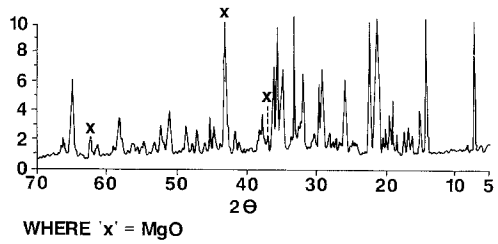

Figure 8 XRD pattern of phosphorreslerite.

amorphous phase. This might seem to suggest that the reaction occurring can be represented by the equation

$$2MgO + Al(H_2PO_4)_3 \xrightarrow{+H_2O} 2MgHPO_4 \cdot 3H_2O + AlPO_4 \cdot nH_2O \quad (3)$$

Equation 3 is, however, incorrect, because a 2:1 mixture of MgO:AOP failed to produce a strong set cement (Figs 2 and 4). It can also be seen from Fig. 4 that there was very little unreacted MgO present in the set cement until a molar ratio in excess of 3:1 was used. Furthermore, the amount of newberyite formed reached a peak at a 4:1 MgO:AOP molar ratio. Beyond 4:1, the extra MgO appeared, unreacted, in the product. It is evident, therefore that an excess of around 2 mol MgO was necessary to push the reaction to completion. The reaction route for a set cement may therefore be modified to

$$4MgO + Al(H_2PO_4)_3 \xrightarrow{+H_2O} MgHPO_4 \cdot 3H_2O + AlPO_4 \cdot nH_2O + 2MgO \quad (4)$$

Further reference to Fig. 4 shows that Equation 4 is still not a completely accurate description of the reaction. As mentioned above, there is no unreacted MgO detected in a cement formed by a 3:1 MgO:AOP mixture, while Equation 4 suggests that there should be. Hence it is proposed that this "missing" magnesium is contained in the amorphous material, which must therefore be a phase in the Al_2O_3–MgO–P_2O_5–H_2O system.

Varying quantities of magnesium can be accommodated in the amorphous material, saturation being reached when the atomic ratio in this phase is around Mg:Al = 1:1. The exact amount of magnesium which appears in the form of newberyite, magnesia or in the amorphous phase depends on a number of factors, such as the molar ratio MgO:AOP, the particle size and reactivity of the starting materials, and the intimacy and duration of mixing.

Hence the most accurate equation for the reaction is

$$pMgO + Al(H_2PO_4)_3 \xrightarrow{+H_2O} qMgHPO_4 \cdot 3H_2O + [\tfrac{1}{2}Al_2O_3 - rMgO - \tfrac{1}{2}P_2O_5 - sH_2O] + tMgO \quad (5)$$

where $r \leqslant 1$, $t = 0$ until $p > 3$, and p must $\geqslant 2$ to produce a set cement.

4.3. Microstructure of the reaction product

The set cement was examined using a scanning electron microscope with EDAX facilities, in an attempt to gain further understanding both of the overall microstructure, and of the stoichiometry of the amorphous phase(s).

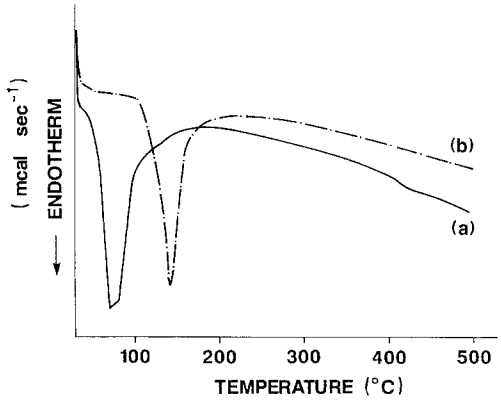

Figure 9 DSC curve of phosphorreslerite crystals (a) freshly grown, (b) after 2 wk at ambient conditions.

A sample was prepared by mixing MgO and AOP in the molar ratio 4:1, and allowing it to set. The cement was then left to harden at ambient temperature and humidity. After 7 days, the sample was broken in two, and the fracture surfaces examined by SEM. Figs 10 to 13 are electron micrographs produced from this examination. In Fig. 10, a low-magnification micrograph, crystalline regions are clearly visible. A considerably magnified view of the region slightly above centre in Fig. 10 is shown in Fig. 11, with extensive columnar crystal growth clearly evident. Areas such as these are attributed to the crystalline material detected by XRD, namely $MgHPO_4 \cdot 3H_2O$. Analysis by EDAX supported this view since the material contained magnesium and phosphorus, but virtually no aluminium. It is believed that the sample did not cleave through these crystals, but rather that the crystals grew in a pore in the sample, through which the fracture surface subsequently passed. Because the crystalline material is hydrated, it could be that there was some free water contained in the pore after initial setting of the cement, and the newberyite gradually grew into this region. This would be similar to the through-solution route by which some hydrate crystals are found to form in ordinary Portland cement [24], other magnesia–phosphate cements [12], and high alumina cements [25].

Fig. 12 shows a degree of crystallinity also, with faceted, flat surfaces, cleavage planes and steps in the surfaces. On analysis, this material was found to consist principally of magnesium, with very little aluminium or phosphorus present. Hence it was concluded that areas such as these were simply inclusion of unreacted MgO.

The left-hand side of Fig. 13, and the edges around Fig. 10 shows the morphology typical of much of the fracture surfaces. There are no smooth areas, no evidence of faceting, and no other indications of crystallinity. It seems probable that this is the amorphous material detected by XRD. It was hoped to use EDAX in a semi-quantitative manner to indicate something of the stoichiometry of this amorphous material. However, the nature of fractured cement surfaces is such that meaningful results are often hard to obtain

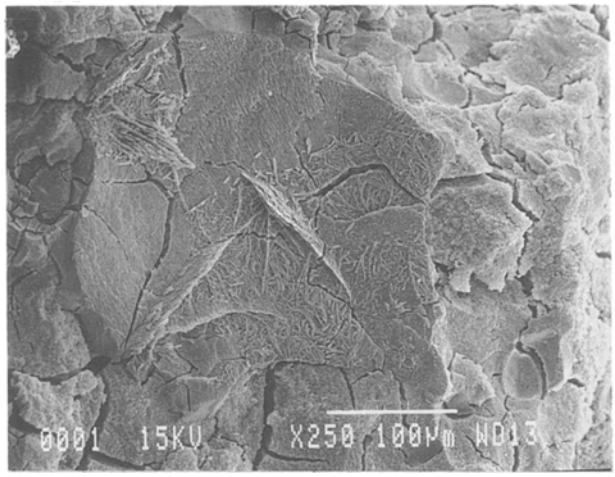

Figure 10.

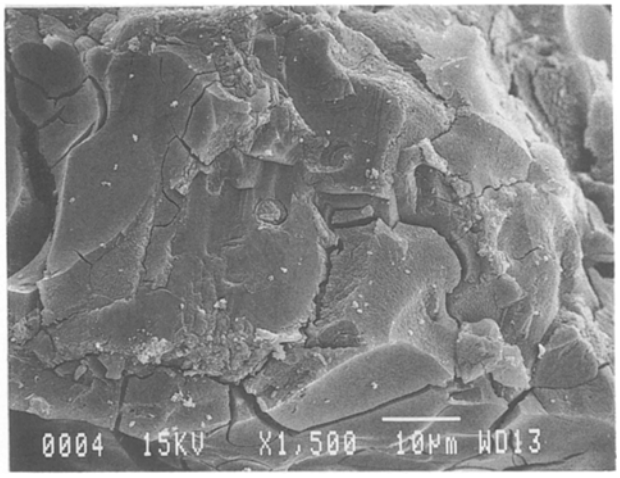

Figure 12.

Figure 10 to 13 Scanning electron micrographs, showing a fracture surface of a cement containing newberyite.

(take-off angles and shadowing effects are difficult to estimate accurately due to sample morphology, for example). Hence, only very general conclusions can be drawn from these EDAX studies. The results did, however, strongly suggest two points:

(i) there is a wide range of composition in the amorphous material suggesting a random, three-dimensional network.

(ii) substantial amounts of magnesium are contained in the amorphous material, in support of the hypothesis advanced in the preceding section.

5. Reaction between MgO + "in-house" acids

5.1. The preparation of in-house acid sources

In an attempt to reduce the water content and hence obtain a better green strength of these phosphate cements, an "in-house" aluminium acid phosphate has been developed. By combining phosphoric acid and gibbsite in the appropriate molar proportions, a viscous acid source was obtained which contained considerably less water than commercially available AOP. To calculate a figure for the nominal concentration of $Al(H_2PO_4)_3$ in these acids, it is assumed that all the gibbsite reacts to form $Al(H_2PO_4)_3$. Thus, if

P:Al = 3:1

$$6H_3PO_4(aq) + 2Al(OH)_3 \rightarrow 2Al(H_2PO_4)_3 + 6H_2O \quad (6)$$

From this assumption the reaction product formed when gibbsite reacts with 85.3% wt/wt phosphoric acid is a nominally 75% wt/wt solution at $Al(H_2PO_4)_3$ in water. Commercially available AOP acids are generally ~50% wt/wt solutions, calculated by the same method.

If the ratio of phosphoric acid:gibbsite is higher than that given by Equation 6, it is assumed that any extra H_3PO_4 remains unreacted. Thus depending on the quantity of H_3PO_4 solution used, the acid can be said to consist of:

P:Al > 3, a solution of AOP in H_3PO_4 solution;

P:Al = 3, a solution of AOP in H_2O;

P:Al < 3, mixtures were found to be only metastable, and to harden on storage. This observation agrees with that reported by Cassidy [2].

It is likely that the assumption that all the gibbsite reacts to form $Al(H_2PO_4)_3$ is an oversimplification. It was found, however, that the acid source produced from a 3:1 P:Al ratio, when dried at a moderate

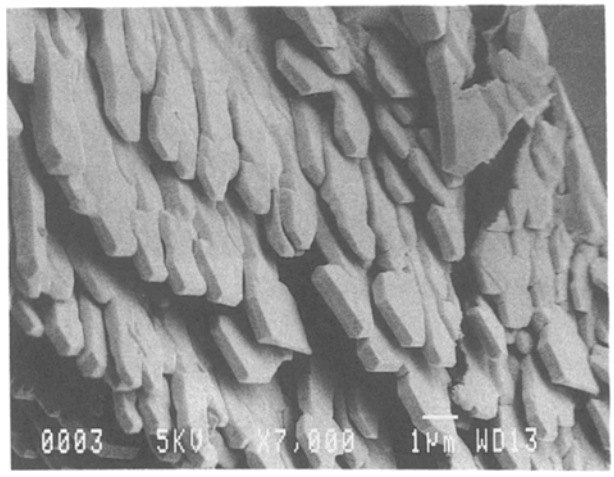

Figure 11.

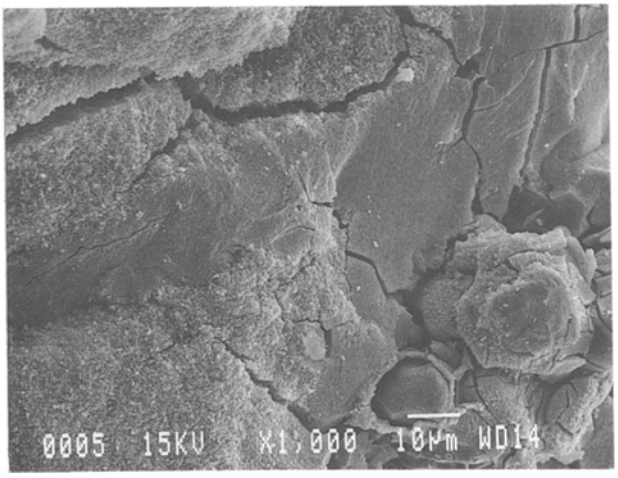

Figure 13.

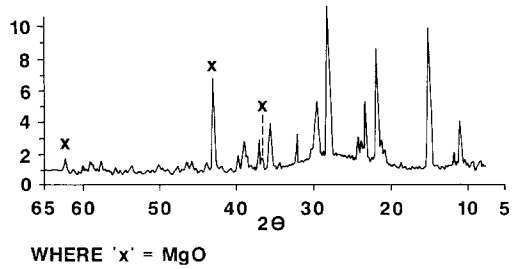

Figure 14 XRD pattern of hayesite.

temperature (e.g. 150° C for 24 h) formed crystals which were shown by XRD to be entirely $Al(H_2PO_4)_3$.

This "in-house" acid source was diluted with water to produce a family of acids with a wide range of concentrations and compositions.

5.2. Characterization of the reaction products

As with commercial AOP, in-house acids can be combined with MgO to produce solid products, via a strongly exothermic reaction.

When an acid of similar composition and water content to commercial AOP is combined with MgO, the resulting cement contains newberyite and a quantity of amorphous material. This is identical to the product formed by combining commercial AOP + MgO.

If, however, an acid with a lower water content is combined with MgO, it is often the case that a different crystalline phase to newberyite is formed, alongside a quantity of amorphous material. Because newberyite is a trihydrate, it is to be expected that its formation is inhibited when there is little water available. What is surprising, however, is that the crystalline material formed by this low water content acid has not previously been reported in the scientific literature. Because this is the case, further details regarding the unidentified material, which has provisionally been dubbed "hayesite", are given below.

The reaction products identified by XRD when MgO was added to in-house acids with a range of compositions, are listed in Table V. In addition to excess MgO and amorphous material, it can be seen that newberyite, hayesite or a mixture of both phases could be formed.

The XRD pattern of hayesite is shown in Fig. 14. The composition of the reactant mixture which gave rise to Fig. 14 was $Mg:P:Al:H_2O$ = 3.6:4:1:13.5. The sample also contained some unreacted MgO, but not newberyite. The XRD pattern of hayesite is distinct from that of newberyite.

Because this new X-ray pattern had not been reported previously, a second X-ray analysis was performed at AERE, Harwell, UK, using copper radiation with a Siemens kristalloflex 810 Diffrac 11 linked to a D.E.C. computer search–match facility. The XRD data obtained from this equipment are listed in Table VI with the three peaks due to MgO omitted. The *d*-spacings and intensities matched very closely indeed with those obtained on the same material using the Philips diffractometer.

The infrared spectrum of a hayesite-containing sample is shown in Fig. 5c. The sample had a composition of $Mg:P:Al:H_2O$ = 3.6:3:1:5.8. When this spectrum is compared with those of newberyite (Figs 5a and b), it can be seen from the lack of fine structure, especially below 1250 cm^{-1}, that hayesite is somewhat less crystalline than newberyite. The most interesting point about this spectrum, however, is the presence of peaks at ~3400 and 1640 cm^{-1}, clearly confirming that hayesite is a hydrated phase.

DSC and TG curves of a sample (composition $Mg:P:Al:H_2O$ = 3.6:4:1:13.5) containing hayesite are shown in Figs 6c and 7c, respectively. These provide further evidence that hayesite is a hydrate, which loses its water of crystallization at 190 to 200° C. Although a weak, broad endotherm was sometimes observed at 350° C, a more significant endothermic peak was observed at 500° C, which is almost certainly due to dehydroxylation, because it is accompanied by a sharp loss in mass.

When these TG results are compared with those from a sample containing newberyite (Fig. 7b), it is evident that on dehydration at 180 to 200° C, the hayesite-containing sample loses appreciably less mass than the newberyite-containing sample (~8% cf. 20%). This suggests that hayesite is probably a lower hydrate than newberyite, but because of the presence of the amorphous phases, it is not possible to be more quantitative.

Hayesite also remains stable up to a slightly higher temperature than newberyite, which indicates that

TABLE V Crystalline phases produced from "in-house" acids + MgO

Mg	P	Al	H_2O	Reaction product observed
3.0	4	1	13.5	Hayesite (+ some newberyite)
3.6	4	1	13.5	Hayesite
4.5	4	1	13.5	Newberyite (+ some hayesite)
3.6	4	1	44	Newberyite
3.6	4	1	56	Hayesite
3.6	4	1	81	Newberyite
3.6	3	1	5.8	Hayesite
3.0	3	1	5.8	Hayesite
3.6	3	1	21.6	Newberyite
3.6	3	1	41.2	Newberyite

TABLE VI *d*-spacings and relative intensities for hayesite

d (nm)	I/I_0	*d* (nm)	I/I_0
0.8286	45	0.2565	2
0.7568	11	0.2524	15
0.5928	70	0.2460	3
0.4837	4	0.2327	10
0.4328	6	0.2312	12
0.4246	6	0.2273	6
0.4124	45	0.2152	3
0.3847	15	0.2063	6
0.3783	6	0.1986	5
0.3716	8	0.1957	4
0.3202	100	0.1714	3
0.3072	15	0.1650	3
0.3042	20	0.1601	4
0.2961	5	0.1566	4
0.2798	9	0.1539	3
0.2619	4	0.1506	2

the water is bound more strongly than in newberyite. This is consistent with the hypothesis that hayesite may simply be a lower hydrate of magnesium hydrogen phosphate, such as $MgHPO_4 \cdot H_2O$, or $MgHPO_4 \cdot 2H_2O$.

Three alternative possibilities exist for hayesite. It might be a magnesium phosphate hydrate with a different Mg:P ratio from that of newberyite. It could possibly be a polymorphic form of $MgHPO_4 \cdot 3H_2O$. Finally, it might be a magnesium aluminium phosphate hydrate.

We believe that a lower hydrate, perhaps the monohydrate or the dihydrate, of $MgHPO_4$ is the most likely stoichiometry for hayesite. Brushite, $CaHPO_4 \cdot 2H_2O$, is well known. Because a hepta- and a trihydrate exist in the phosphorreslerite–newberyite series, it is feasible that a penta- and mono-hydrate may form under the correct conditions. If the monohydrate exists, it is somewhat surprising that no evidence for it was observed during the dehydration of the trihydrate. In the present study, however, the DSC curve of the heptahydrate indicates the formation of anhydrous $MgHPO_4$ without evidence for the intermediate formation of the trihydrate let alone that of the monohydrate (Fig. 9a). Because of the presence of the amorphous phase in all the samples it is not possible on the basis of the results obtained to distinguish between these possibilities.

6. Conclusions

1. The reaction of MgO and H_3PO_4 yields a product consisting of $Mg(H_2PO_4)_2 \cdot 2H_2O$, which is soluble in water.

2. MgO reacts with commercial $Al(H_2PO_4)_3$ with the evolution of heat to form an insoluble product which is a set cement of moderate strength.

3. The products of this reaction are crystalline newberyite, $MgHPO_4 \cdot 3H_2O$, and an amorphous phase.

4. This amorphous phase is a hydrated form of $AlPO_4$ but almost certainly also contains magnesium.

5. As the molar ratio of MgO:AOP increases, the cement sets faster with a greater evolution of heat.

6. Phosphorreslerite, $MgHPO_4 \cdot 7H_2O$, can be formed in the presence of excess water, but readily transforms into the trihydrate, newberyite, at ambient temperatures.

7. An alternative set of acid sources has been made by dissolving gibbsite in phosphoric acid and adding water. An acid of similar composition and water content to commercial AOP also reacted with MgO to form newberyite, but acids with lower water contents can react to form a new hydrate referred to here as "hayesite".

8. Hayesite is probably a lower hydrate of $MgHPO_4$ than newberyite, perhaps $MgHPO_4 \cdot H_2O$ or $MgHPO_4 \cdot 2H_2O$.

9. These cements, like other magnesia–phosphate cements containing ammonium ions [12], are readily formed by an exothermic, acid–base reaction, leading to the formation of hydrates by a through-solution mechanism involving nucleation and precipitation from the pore fluid.

Acknowledgements

The authors thank colleagues in the Materials Department, THORN EMI Central Research Laboratories especially Mr D. Holtom and Dr S. Soubhi, for their invaluable help and encouragement in this work. They also thank Mr M. Pearce for his help in producing the micrographs.

References

1. W. D. KINGERY, *J. Amer. Ceram. Soc.* **33** (1950) 239.
2. J. E. CASSIDY, *Amer. Ceram. Bull.* **56** (1977) 640.
3. J. ANDO, T. SHINADA and G. HIRAOKA, *Yogya Kyokai Shi* **82** (1974) 644.
4. B. EL-JAZAIRI, *Concrete* **16**(9) (1982) 12.
5. T. SUGAMA and L. E. KUKACKA, *Cem. Concr. Res.* **13** (1983) 407.
6. *Idem, ibid.* **13** (1983) 499.
7. B. E. I. ABDELRAZIG, P. A. SIDDY, J. H. SHARP and B. EL-JAZAIRI, *Proc. Brit. Ceram. Soc.* **35** (1984) 141.
8. B. E. I. ABDELRAZIG and J. H. SHARP, *Cem. Concr. Res.* **15** (1985) 921.
9. S. POPOVICS, N. RAJENDRAN and M. PENKO, *A.C.I. Mater. J.* **84** (1987) 64.
10. B. EL-JAZAIRI, *Concrete* **21**(9) (1987) 25.
11. B. E. I. ABDELRAZIG and J. H. SHARP, *Thermochim. Acta* **129** (1988) 197.
12. B. E. I. ABDELRAZIG, J. H. SHARP and B. EL-JAZAIRI, *Cem. Concr. Res.* **18** (1988) 415; *ibid.* **19** (1989) 247.
13. Joint Committee on Powder Diffraction Standards, Card 4-829 (Pennsylvania, USA).
14. TH. R. HINSCH, *Neues Hahrb. Mineral Monatsh.* **10** (1985) 439.
15. Joint Committee on Powder Diffraction Standards, Card 1-781 (Pennsylvania, USA).
16. S. AHMED, *Pakistan J. Sci. Ind. Res.* **15** (1972) 142.
17. D. J. SUTOR, *Acta Crystallogr.* **23** (1967) 418.
18. S. D. ROSS, "IR Spectra of Minerals", edited by V. C. Farmer (Mineralogical Society, London, 1974) p. 383.
19. F. A. MILLER and C. H. WILKINS, *Anal. Chem.* **24** (1952) 1253.
20. J. R. LEHR, E. H. BROWN, A. W. FRAZIER, J. P. SMITH and R. D. THRASHER, *Chem. Engng Bull.* **6** (1967) 127.
21. Joint Committee on Powder Diffraction Standards, Card 19-761 (Pennsylvania, USA).
22. J. R. VAN WAZER, "Phosphorus and its compounds", Vol. 1 (Interscience, New York, 1958) p. 851.
23. N. S. RASSONSKAYA and O. S. NOVIKOVA, *Russ. J. Inorg. Chem.* **10** (1965) 774.
24. H. M. JENNINGS, in "Advances in Cement Technology", edited by S. N. Ghosh (Pergamon, Oxford, 1983) p. 349.
25. C. BRADBURY, P. M. CALLAWAY and D. D. DOUBLE, *Mater. Sci. Engng* **23** (1976) 43.

Received 7 October 1988
and accepted 24 January 1989